Received: 15 December 2024 | Revised: 15 April 2025 | Accepted: 29 May 2025 | Published online: 13 June 2025

RESEARCH ARTICLE

Medinformatics
2025, Vol. 2(3) 154–166
DOI: 10.47852/bonviewMEDIN52025019

BON VIEW PUBLISHING

Virtual Screening and Molecular Docking Characterization of Isoxazole-Based Small Molecules as Potential Hsp90 Inhibitors: An in Silico Insight

Adam A. Aboalroub[1,*]

[1]*Pharmaceutical Sciences Department, Al-Ahliyya Amman University, Jordan*

Abstract: The heat shock protein 90 (Hsp90) is a chaperone machinery implicated in the activity of hundreds of client proteins. Numerous Hsp90 clients have been involved in cancer initiation, progression, and metastasis. Hsp90 becomes more prone to bind to drug-like small molecules in the cancer milieu. Consequently, modulating Hsp90 activity by such molecules is a promising and growing approach for cancer therapy. Isoxazole-based molecules such as Luminespib have exhibited potent inhibitory impacts on Hsp90 activity in myriad human tumor cell lines. In this work, we applied a computer-based protocol to identify isoxazole derivatives to combat Hsp90 oncogenic activity. Screening the ZINC database revealed that thirty-six isoxazole-based molecules can function as Hsp90 inhibitors. Molecular docking simulation analysis demonstrated that twelve of these ZINC compounds have binding energies ranging from −8.23 to −8.51 kcal/mol, which implies a high binding affinity compared to that of Luminespib, with a binding energy of −8.20 kcal/mol. These compounds bind to Hsp90 via hydrogen bonds and hydrophobic interactions with crucial residues such as Gly97, Asn51, and Lys58. Furthermore, several of these compounds have demonstrated their ability to interact with acidic residues on Hsp90 via electrostatic interactions, forming salt bridges. The compounds identified in this study offer a promising foundation for developing potent Hsp90-targeting anticancer agents. To fully evaluate their efficacy in mitigating cancer cell growth, further investigation in cell-based and *in vivo* models, including optimization of dosing regimens, is warranted.

Keywords: drug-like molecules, Hsp90, *in silico* approaches, molecular docking analysis, isoxazole

1. Introduction

Cancer, a notorious group of diseases, stands as the second leading cause of death globally. It is characterized by irregular and uncontrolled cell proliferation that extends to impact normal cells [1]. The severity of this pathological condition has prompted research to identify protein targets for cancer treatment [2]. Myriad proteins have been implicated in cancer's initiation, progression, and spread [3]. One significant protein group is the ATP-dependent heat shock proteins (Hsps), particularly the most abundant one, a 90 kDa molecular chaperone called Hsp90 [4]. Hsp90 is involved in all stages of cancer development, from tumor initiation to invasion and metastasis [4–6]. Hsp90 plays a vital role in the activity of hundreds of client proteins under normal and pathological conditions [5]. Hsp90 utilizes ATP hydrolysis to assist in protein folding and maintain protein stability and conformation [6]. Hsp90-dependent proteins are involved in essential cellular processes, including DNA repair and signal transduction pathways [1]. Conversely, the dysregulation of Hsp90 clients has been linked to the development of several pathological conditions, including neurodegenerative diseases and cancer [7]. In cancer, Hsp90 ensures the stability of several oncogenic proteins, whose activities contribute to tumor cell survival and metastasis [8]. Notably, the overexpression of Hsp90 in tumor cells, which is 2–10 times greater than that in normal cells, leads to elevated levels of the client proteins and, consequently, tumor cell growth [9]. Accordingly, Hsp90 is considered a valuable target for cancer treatment [6]. Hsp90 is a homodimeric protein that consists of three structural domains: the N-terminal domain (N-Hsp90), the C-terminal domain (C-Hsp90), and the middle domain (M-Hsp90) [4, 10]. The N-terminal domain of Hsp90, housing the ATP-binding pocket, is a primary target for inhibitors designed to disrupt the protein's ATPase activity [10]. Over eighteen Hsp90 inhibitors have entered clinical trials [11]. These inhibitors, though not yet approved for market, have shown the ability to bind to N-Hsp90 and impact the multiplication of cancer cells by inducing G1-G2 arrest and apoptosis [12].

Heterocyclic compounds are prevalent in bioactive molecules and offer a diverse range of therapeutic properties, including antibacterial, antiviral, antifungal, and anti-inflammatory activities [13, 14]. Similarly, the synthetic analogs of these compounds have demonstrated a wide range of biological activities, often

*Corresponding author: Adam A. Aboalroub, Pharmaceutical Sciences Department, Al-Ahliyya Amman University, Jordan. Email: Jordan.a.aburoub@ammanu.edu.jo

surpassing their natural counterparts in terms of potency, selectivity, and pharmacokinetic properties [15]. These molecules exert biological effects through various mechanisms, including inhibiting protein expression by binding to DNA or RNA, disrupting signaling pathways by interfering with protein-protein interactions, and modulating protein activity through competitive or non-competitive inhibition [16, 17]. Numerous heterocyclic compounds, such as derivatives based on purine, pyrazole, triazine, quinoline, coumarin, and isoxazole, have been developed to regulate Hsp90 chaperone activity [18–21].

Isoxazole is a five-membered heterocyclic compound containing three carbon atoms, one oxygen atom, and one nitrogen atom at positions 1 and 2 [22]. Isoxazole-based Hsp90 inhibitors demonstrate promising efficacy, favorable pharmacokinetic properties, and low toxicity [8, 23, 24]. For example, N-(isoxazole-5-yl) amides have demonstrated distinct pharmacokinetic profiles and potent antitumor activity in both *in vitro* and *in vivo* studies [25]. Notably, VER-50589, an isoxazole-containing compound discovered through high-throughput screening and structure-based design, exhibited comparable inhibitory activity against Hsp90 to the clinically approved drug 17-AAG [23, 26]. Furthermore, VER-50589 demonstrated improved cellular uptake and favorable pharmacokinetic and pharmacodynamic properties, rivaling the lead Hsp90 inhibitor CCT018159 [14, 25]. Luminespib (AUY922), another isoxazole-derived compound, has exhibited high selectivity and potent inhibitory activity against Hsp90 in various human tumor cell lines [27, 28]. Luminespib mechanism of action involves inhibiting Hsp90's ATPase activity, which triggers the degradation of client proteins and disrupts critical signaling pathways for tumor growth, survival, and metastasis (e.g., PI3K/AKT/mTOR, RAF/MEK/ERK) [27, 29]. Luminespib exhibits nanomolar potency *in vitro*, effectively reducing cancer cell viability through apoptosis [27]. In preclinical studies, Luminespib inhibited tumor growth and displayed synergistic potential in combination with other chemotherapeutic or targeted agents [27, 29]. Clinical development in Phase I and II trials has shown manageable toxicity but limited monotherapy efficacy, driving ongoing research into combination treatment strategies [27, 29].

Computer-aided drug design (CADD) is a valuable tool for identifying drug-like small molecules and exploring their potential biological activities [29–31]. The current study utilized *in silico* methods to identify potential Hsp90 inhibitors, leveraging the promising therapeutic potential of targeting Hsp90 in cancer treatment. The ZINC database was screened for isoxazole-containing compounds using the Expasy Swiss Similarity platform, employing Luminespib as a reference. A rigorous filtering process based on drug-likeness, pharmacokinetics, and physicochemical properties narrowed the initial 400 candidates to 36. To assess the binding potential of these compounds to Hsp90, online prediction servers (SwissTargetPrediction, Way2drug, SuperPred, SEA) were utilized. Additionally, molecular docking simulations were performed using SwissDock and AutoDock Vina 1.2.0 to investigate binding affinities and interactions with Hsp90. The selected molecules exhibited a strong binding affinity to Hsp90, with twelve compounds demonstrating binding energies (−8.23 to −8.51 kcal/mol) surpassing that of Luminespib (−8.20 kcal/mol). These compounds formed hydrogen bonds and hydrophobic interactions with key Hsp90 residues, including Gly97, Asn51, and Lys58. Additionally, several compounds interacted electrostatically with acidic Hsp90 residues, forming salt bridges. Further optimization of these ZINC compounds could lead to the discovery of potent Hsp90-targeting anticancer agents.

2. Materials and Methods

2.1. Ligand screening and selection

SwissSimilarity is an online tool that provides valuable information for conducting virtual screenings of bioactive molecules in chemical libraries [32, 33]. This work used this platform to screen for the target isoxazole derivatives using Luminespib as a control molecule. First, the Simplified Molecular Input Line Entry (SMILES) format of the control compound was retrieved from the PubChem database to be entered into the SwissSimilarity text box. The drug-like option was selected as the class of compound libraries to screen for the target molecules, and the 2D path-based FP2 fingerprint screening method was selected to search for the target compounds in the ZINC 20 database [32]. The top 400 ranked compounds were filtered based on Lipinski's "rule of five" (RO5) and drug and lead-likeness information using the Expasy SwissADME web service. The inclusion criteria for RO5 included the following: a molecular mass < 500 Da, H-bond donors (HBDs) ≥ 5, H-bond acceptors (HBAs) ≥ 10, rotatable bonds (RBs) ≥ 10, and an octanol-water partition coefficient (CLogP) ≥ 5 [34]. Drug-likeness and lead-likeness properties of the selected compounds were determined according to established medicinal chemistry rules (Veber, Ghose, Egan, and Lipinski) using the Expasy SwissADME web service [35].

2.2. Prediction of ligand binding to Hsp90

The potential binding of Hsp90 to isoxazole compounds was explored using online prediction tools, including SwissTargetPrediction [36], SuperPred 3.0 [37], prediction of activity spectra for substances (PASS) [38], and similarity ensemble approach (SEA) [39]. These platforms leverage ligand similarity to predict potential targets accurately. The SMILES files of the selected isoxazole compounds were input into these web tools to assess their interaction with Hsp90.

2.3. Molecular docking simulation

Molecular docking simulations were employed to investigate the binding of potential inhibitors to Hsp90 at the atomic level. This computational technique provides valuable insights into the mode of interaction between ligands and target biomolecules [40]. By leveraging the known structure of Hsp90, the docking simulations predicted the preferred binding sites and affinities of the selected compounds [41]. Molecular docking studies were conducted to investigate the interaction of selected ZINC molecules with human Hsp90 (PDB ID: 6LTI). These studies utilized the Expasy SwissDock online server, with Luminespib serving as a control. The molecular docking workflow began with the crystal structure of the Hsp90-Luminespib complex (PDB ID: 6LTI; Figure 1) as the protein target. SwissDock [42] was used to define the Luminespib binding site, and Chimera [43] was employed for protein preparation. The protein crystal structure was prepared in Chimera by removing water molecules and nonstandard residues (including the original ligand), followed by

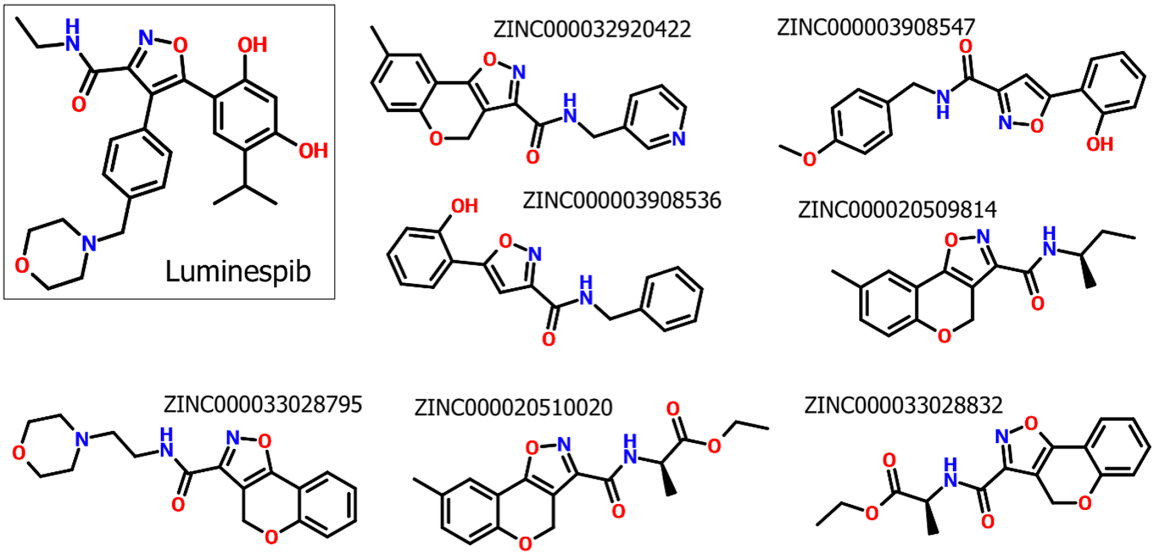

Figure 1. The chemical structures of Luminespib and the selected top-ranked ZINC molecules

energy minimization and the addition of hydrogens and charges. Since the target ligands were obtained from the ZINC database in ready-to-dock 3D format [44], they required no further processing. Molecular docking simulations were conducted using the SwissDock online server with the following predefined parameters: WANTEDCONFS (number of conformations generated) = 5000; NBFACTSEVAL (number of evaluations of the force field) = 5000; NBSEEDS (number of initial random positions) = 250; SDSTEPS (number of steps for stochastic dynamics) = 100; ABNRSTEPS (number of steps for ABNR minimization) = 250; CLUSTERINGRADIUS (clustering radius in Å) = 2.0; and MAXCLUSTERSIZE (maximum cluster size) = 8 [42]. Visualization of the docking results was performed using UCSF Chimera. The docking procedure was validated through redocking of Luminespib to the ATP-binding site of N-Hsp90. The reliability of the docking results was subsequently assessed using AutoDock Vina 1.2.0, a widely used tool for predicting ligand-protein binding affinities and binding sites. Using a docking grid of 20 Å x 20 Å x 20 Å centered at (33, −14, −20) Å, ZINC compounds were docked against the N-terminal domain of human Hsp90 (PDB ID: 6LTI). The docking simulations were conducted with default parameters, setting the exhaustiveness to 64. UCSF Chimera was used for analysis and visualization.

2.4. *In silico* cytotoxicity prediction in tumor cell lines

In silico prediction of cytotoxicity in tumor cell lines offers a time- and cost-effective strategy for screening potential anticancer agents and evaluating their safety. Computational methods, such as the CLC-Pred 2.0 platform (Cell Line Cytotoxicity Predictor), enable the prediction of compound cytotoxicity in non-transformed and transformed (cancer) cell lines using structural formulas as input [45]. CLC-Pred 2.0 employs Quantitative Structure-Activity Relationship (QSAR) models, trained on experimental cytotoxicity data from a range of cell lines, to predict activity by comparing the structural features of the query compound with those in its database. The potential cytotoxicity of the selected top-ranked molecules against cell lines was predicted using CLC-Pred 2.0 (https://www.way2drug.com/Cell-line) by inputting their SMILES representations.

3. Results and Discussion

Computer-aided drug discovery is an emerging and evolving research domain that seeks to determine and characterize molecules with favorable biological activity [46]. Breakthroughs in machine learning technologies have made this approach valuable and reliable for predicting and validating the biological functions of chemical compounds [30]. In this work, *in silico* approaches were utilized to find isoxazole-containing molecules as potential inhibitors of the Hsp90 ATPase activity. Employing bioactive molecules as protein inhibitors is a promising protocol for cancer-based therapies. Compared to large-molecule drugs such as monoclonal antibodies and polypeptides, small molecule drugs are inexpensive, compliant, and have good pharmacokinetic properties [47]. Moreover, it covers numerous targets, including kinases, proteasomes, and several regulatory proteins. This study primarily focused on *in silico* screening and molecular docking to identify promising scaffolds exhibiting favorable binding affinities and interaction profiles with the Hsp90 ATP-binding site. While these computational methods provide a valuable initial assessment, robust validation of the obtained results through *in vitro* biochemical assays, cell-based studies, and comprehensive pharmacokinetic and pharmacological evaluations is warranted.

3.1. Isoxazole screening and selection

Operating the Expasy SwissSimilarity platform, a screen of the ZINC database was executed to identify small molecules with structural similarity to Luminespib, a known Hsp90 inhibitor. Luminespib, an isoxazole derivative, functions as an Hsp90 ATPase inhibitor by targeting the ATP-binding pocket within the N-terminal domain [29]. Compared to established Hsp90 inhibitors like 17-AAG, Luminespib demonstrates superior *in vitro* and *in vivo* inhibitory activity, selectivity, and pharmacokinetic properties [29, 48]. Luminespib-induced inhibition of Hsp90 can lead to cancer cell proliferation arrest, apoptosis, and depletion of dependent proteins [29, 49]. Luminespib was used as a template molecule in similarity-based screening, which assumes that structurally similar molecules often exhibit analogous biological activities [49, 50]. The ZINC database comprises hundreds of

Table 1. The selected ZINC compounds and Luminespib, molecular formula, molecular weight, and SMILE files

ZINC Code	Molecular Formula	MW (g/mol)	SMILE
ZINC000020510095	$C_{20}H_{18}N_2O_3$	334.37	C[C@H](NC(=O)C1=NOC2=C1COC1=CC=C(C)C=C21)C1=CC=CC=C1
ZINC000035477380	$C_{15}H_{14}N_2O_3$	258.27	CCNC(=O)C1=NOC2=C1COC1=CC=C(C)C=C21
ZINC000020509814	$C_{16}H_{18}N_2O_3$	286.33	CC[C@@H](C)NC(=O)C1=NOC2=C1COC1=CC=C(C)C=C21
ZINC000020509816	$C_{16}H_{18}N_2O_3$	286.33	CC[C@H](C)NC(=O)C1=NOC2=C1COC1=CC=C(C)C=C21
ZINC000032920495	$C_{19}H_{16}N_2O_3$	320.34	CC1=CC=C2OCC3=C(ON=C3C(=O)NCC3=CC=CC=C3)C2=C1
ZINC000020509949	$C_{20}H_{18}N_2O_3$	334.37	CC1=CC=C(CNC(=O)C2=NOC3=C2COC2=CC=C(C)C=C32)C=C1
ZINC000035477309	$C_{15}H_{16}N_2O_3$	272.30	CC[C@@H](C)NC(=O)C1=NOC2=C1COC1=CC=CC=C21
ZINC000035477310	$C_{15}H_{16}N_2O_3$	272.30	CC[C@H](C)NC(=O)C1=NOC2=C1COC1=CC=CC=C21
ZINC000015673863	$C_{17}H_{20}N_2O_3$	300.35	CCCN(CCC)C(=O)C1=NOC2=C1COC1=CC=CC=C21
ZINC000035537827	$C_{16}H_{16}N_2O_4$	300.31	CC1=CC=C2OCC3=C(ON=C3C(=O)N3CCOCC3)C2=C1
ZINC000020484607	$C_{15}H_{16}N_2O_3$	272.30	CCCCNC(=O)C1=NOC2=C1COC1=CC=CC=C21
ZINC000020484604	$C_{14}H_{14}N_2O_4$	274.27	COCCNC(=O)C1=NOC2=C1COC1=CC=CC=C21
ZINC000020484847	$C_{18}H_{14}N_2O_3$	306.32	O=C(NCC1=CC=CC=C1)C1=NOC2=C1COC1=CC=CC=C21
ZINC000020509776	$C_{18}H_{20}N_2O_3$	312.36	CC1=CC=C2OCC3=C(ON=C3C(=O)NC3CCCCC3)C2=C1
ZINC000003908545	$C_{18}H_{16}N_2O_3$	308.33	C[C@H](NC(=O)C1=NOC(=C1)C1=CC=CC=C1O)C1=CC=CC=C1
ZINC000003908546	$C_{18}H_{16}N_2O_3$	308.33	C[C@@H](NC(=O)C1=NOC(=C1)C1=CC=CC=C1O)C1=CC=CC=C1
ZINC000020901917	$C_{15}H_{14}N_2O_4$	286.28	O=C(N1CCOCC1)C1=NOC2=C1COC1=CC=CC=C21
ZINC000020484748	$C_{18}H_{13}ClN_2O_3$	340.76	ClC1=CC=C(CNC(=O)C2=NOC3=C2COC2=CC=CC=C32)C=C1
ZINC000020510020	$C_{17}H_{18}N_2O_5$	330.34	CCOC(=O)[C@@H](C)NC(=O)C1=NOC2=C1COC1=CC=C(C)C=C21
ZINC000020510023	$C_{17}H_{18}N_2O_5$	330.34	CCOC(=O)[C@H](C)NC(=O)C1=NOC2=C1COC1=CC=C(C)C=C21
ZINC000003908532	$C_{17}H_{13}FN_2O_3$	312.30	OC1=CC=CC=C1C1=CC(=NO1)C(=O)NCC1=CC=C(F)C=C1
ZINC000003908564	$C_{14}H_{16}N_2O_3$	260.29	CCN(CC)C(=O)C1=NOC(=C1)C1=CC=CC=C1O
ZINC000003908535	$C_{18}H_{16}N_2O_3$	308.33	OC1=CC=CC=C1C1=CC(=NO1)C(=O)NCCC1=CC=CC=C1
ZINC000033028831	$C_{16}H_{16}N_2O_5$	316.31	CCOC(=O)[C@@H](C)NC(=O)C1=NOC2=C1COC1=CC=CC=C21
ZINC000033028832	$C_{16}H_{16}N_2O_5$	316.31	CCOC(=O)[C@H](C)NC(=O)C1=NOC2=C1COC1=CC=CC=C21
ZINC000033028795	$C_{17}H_{19}N_3O_4$	329.35	O=C(NCCN1CCOCC1)C1=NOC2=C1COC1=CC=CC=C21
ZINC000003908558	$C_{14}H_{16}N_2O_3$	260.29	CC(C)CNC(=O)C1=NOC(=C1)C1=CC=CC=C1O
ZINC000013119868	$C_{14}H_{16}N_2O_3$	260.29	CC[C@@H](C)NC(=O)C1=NOC(=C1)C1=CC=CC=C1O
ZINC000013119870	$C_{14}H_{16}N_2O_3$	260.29	CC[C@H](C)NC(=O)C1=NOC(=C1)C1=CC=CC=C1O
ZINC000032920422	$C_{18}H_{15}N_3O_3$	321.33	CC1=CC=C2OCC3=C(ON=C3C(=O)NCC3=CC=CN=C3)C2=C1
ZINC000003908529	$C_{18}H_{16}N_2O_3$	308.33	CN(CC1=CC=CC=C1)C(=O)C1=NOC(=C1)C1=CC=CC=C1O
ZINC000003908536	$C_{17}H_{14}N_2O_3$	294.30	OC1=CC=CC=C1C1=CC(=NO1)C(=O)NCC1=CC=CC=C1
ZINC000003908554	$C_{14}H_{16}N_2O_3$	260.29	CCCCNC(=O)C1=NOC(=C1)C1=CC=CC=C1O
ZINC000003908038	$C_{14}H_{16}N_2O_3$	260.29	CCCNC(=O)C1=NOC(=C1)C1=CC=CC=C1OC
ZINC000047528273	$C_{13}H_{11}F_3N_2O_3$	300.23	COC1=CC=CC=C1C1=CC(=NO1)C(=O)NCC(F)(F)F
ZINC000003908547	$C_{18}H_{16}N_2O_4$	324.33	COC1=CC=C(CNC(=O)C2=NOC(=C2)C2=CC=CC=C2O)C=C1

millions of commercially available synthesized organic molecules ranging in size from 50 to 1000 Da [44]. A screen of the ZINC database for molecules similar to Luminespib yielded 400 potential candidates as Hsp90 inhibitors. These candidates were then subjected to a shortlisting process involving Lipinski's Rule of Five (RO5) and evaluating their pharmacokinetic and physicochemical properties, drug-likeness, and medicinal chemistry using the Expasy SwissADME website. This process resulted in the selection of 36 potential Hsp90 inhibitors with promising potential for further research and development (Table 1 and Figure 1). ChemDraw 3D Ultra version 19.0.0.22 was used to generate the chemical structures of these molecules.

Luminespib is a monocarboxylic acid amide containing an isoxazole ring substituted with two aryl groups at positions 4 and 5 [29]. Similarly, the selected ZINC molecules are based on the isoxazole scaffold, with diverse functional groups attached to the ring (Figure 1). In agreement with Lipinski's RO5, the selected molecules demonstrated favorable drug-like properties, with molecular weights below 500 Da (ranging from 258.27 to 340.76 Da) and acceptable numbers of hydrogen bond donors and acceptors (Tables 1 and 2). These properties are essential for optimal drug absorption and minimize potential interactions. To enhance flexibility and facilitate binding to the target protein, the selected molecules exhibited fewer than ten rotatable bonds (Table 2). Furthermore, the selected molecules adhered to drug-likeness and lead-likeness criteria without violating any of the established standards (Table 2). Drug solubility is a critical factor for achieving adequate pharmacological responses [51]. The selected molecules demonstrated solubility within the moderate to soluble range, as assessed by SwissADME data. The topological polar surface area (TPSA) quantifies the molecular polarity result from polar atoms like sulfur, nitrogen, and oxygen [31]. TPSA is a crucial factor influencing ligand solubility in lipids and provides valuable insights into ligand-protein interactions. Most selected compounds exhibited TPSA values within the optimal 60–140 $Å^2$ range, suggesting favorable oral absorption. *Lipophilicity* is a crucial drug property influencing uptake and metabolism [52, 53]. The selected compounds demonstrated favorable lipophilicity profiles, with LogP values below 5, indicating good permeability across biological membranes.

Table 2. Physicochemical properties, drug-likeness, and binding potential of the selected compounds

	Physicochemical Properties							Drug-Likeness				Hsp90 Binding Prediction			
Compound	HBD	HBA	NRB	Log P	TPSA (Å²)	Log S	Solubility	Lipinski	Ghose	Veber	Egan	SuperPred	PASS	Swiss	SEA
ZINC000020510095	1	4	4	3.43	64.36	−4.32	Mod. Sol.	Yes	Yes	Yes	Yes	Yes	Yes	Yes	Yes
ZINC000035477380	1	4	3	2.23	64.36	−2.88	Soluble	Yes	Yes	Yes	Yes	Yes	Yes	Yes	Yes
ZINC000020509814	1	4	4	2.87	64.36	−3.55	Soluble	Yes	Yes	Yes	Yes	Yes	Yes	Yes	Yes
ZINC000020509816	1	4	4	2.86	64.36	−3.55	Soluble	Yes	Yes	Yes	Yes	Yes	Yes	Yes	Yes
ZINC000032920495	1	4	4	3.14	64.36	−4	Mod. Sol.	Yes	Yes	Yes	Yes	Yes	Yes	Yes	Yes
ZINC000020509949	1	4	4	3.5	64.36	−4.3	Mod. Sol.	Yes	Yes	Yes	Yes	Yes	Yes	Yes	Yes
ZINC000035477309	1	4	4	2.53	64.36	−3.25	Soluble	Yes	Yes	Yes	Yes	Yes	Yes	Yes	Yes
ZINC000035477310	1	4	4	2.54	64.36	−3.25	Soluble	Yes	Yes	Yes	Yes	Yes	Yes	Yes	Yes
ZINC000015673863	0	4	6	3.03	55.57	−3.67	Soluble	Yes	Yes	Yes	Yes	Yes	Yes	Yes	Yes
ZINC000035537827	0	5	2	1.9	64.8	−2.8	Soluble	Yes	Yes	Yes	Yes	Yes	Yes	Yes	Yes
ZINC000020484607	1	4	5	2.55	64.36	−3.14	Soluble	Yes	Yes	Yes	Yes	Yes	Yes	Yes	Yes
ZINC000020484604	1	5	5	1.6	73.59	−2.27	Soluble	Yes	Yes	Yes	Yes	Yes	Yes	Yes	Yes
ZINC000020484847	1	4	4	2.82	64.36	−3.71	Soluble	Yes	Yes	Yes	Yes	Yes	Yes	Yes	Yes
ZINC000020509776	1	4	3	3.26	64.36	−4.05	Mod. Sol.	Yes	Yes	Yes	Yes	Yes	Yes	Yes	Yes
ZINC000003908545	2	4	5	2.81	75.36	−3.97	Soluble	Yes	Yes	Yes	Yes	Yes	Yes	Yes	Yes
ZINC000003908546	2	4	5	2.83	75.36	−3.97	Soluble	Yes	Yes	Yes	Yes	Yes	Yes	Yes	Yes
ZINC000020901917	0	5	2	1.51	64.8	−2.49	Soluble	Yes	Yes	Yes	Yes	Yes	Yes	Yes	Yes
ZINC000020484748	1	4	4	3.35	64.36	−4.3	Mod. Sol.	Yes	Yes	Yes	Yes	Yes	Yes	Yes	Yes
ZINC000020510020	1	6	6	2.32	90.66	−3.24	Soluble	Yes	Yes	Yes	Yes	Yes	Yes	Yes	Yes
ZINC000020510023	1	6	6	2.36	90.66	−3.24	Soluble	Yes	Yes	Yes	Yes	Yes	Yes	Yes	Yes
ZINC000003908532	2	5	5	2.96	75.36	−3.81	Soluble	Yes	Yes	Yes	Yes	Yes	Yes	Yes	Yes
ZINC000003908564	1	4	5	2.13	66.57	−2.94	Soluble	Yes	Yes	Yes	Yes	Yes	Yes	Yes	Yes
ZINC000003908535	2	4	6	2.81	75.36	−3.94	Soluble	Yes	Yes	Yes	Yes	Yes	Yes	Yes	Yes
ZINC000033028831	1	6	6	1.96	90.66	−2.94	Soluble	Yes	Yes	Yes	Yes	Yes	Yes	Yes	Yes
ZINC000033028832	1	6	6	2.03	90.66	−2.94	Soluble	Yes	Yes	Yes	Yes	Yes	Yes	Yes	Yes
ZINC000033028795	1	6	5	1.39	76.83	−2.43	Soluble	Yes	Yes	Yes	Yes	Yes	Yes	Yes	Yes
ZINC000003908558	2	4	5	2.31	75.36	−3.2	Soluble	Yes	Yes	Yes	Yes	Yes	Yes	Yes	Yes
ZINC000013119868	2	4	5	2.34	75.36	−3.2	Soluble	Yes	Yes	Yes	Yes	Yes	Yes	Yes	Yes
ZINC000013119870	2	4	5	2.33	75.36	−3.2	Soluble	Yes	Yes	Yes	Yes	Yes	Yes	Yes	Yes
ZINC000032920422	1	5	4	2.4	77.25	−3.33	Soluble	Yes	Yes	Yes	Yes	Yes	Yes	Yes	Yes
ZINC000003908529	1	4	5	2.72	66.57	−3.83	Soluble	Yes	Yes	Yes	Yes	Yes	Yes	Yes	Yes
ZINC000003908536	2	4	5	2.63	75.36	−3.66	Soluble	Yes	Yes	Yes	Yes	Yes	Yes	Yes	Yes
ZINC000003908554	2	4	6	2.27	75.36	−3.09	Soluble	Yes	Yes	Yes	Yes	Yes	Yes	Yes	Yes
ZINC000003908038	1	4	6	2.38	64.36	−3.07	Soluble	Yes	Yes	Yes	Yes	Yes	Yes	Yes	Yes
ZINC000047528273	1	7	6	2.69	64.36	−3.41	Soluble	Yes	Yes	Yes	Yes	Yes	Yes	Yes	Yes
ZINC000003908547	2	5	6	2.63	84.59	−3.71	Soluble	Yes	Yes	Yes	Yes	Yes	Yes	Yes	Yes
Luminespib	3	7	8	3.77	108.06	−4.78	Mod. Sol.	Yes	Yes	Yes	Yes	Yes	Yes	Yes	Yes

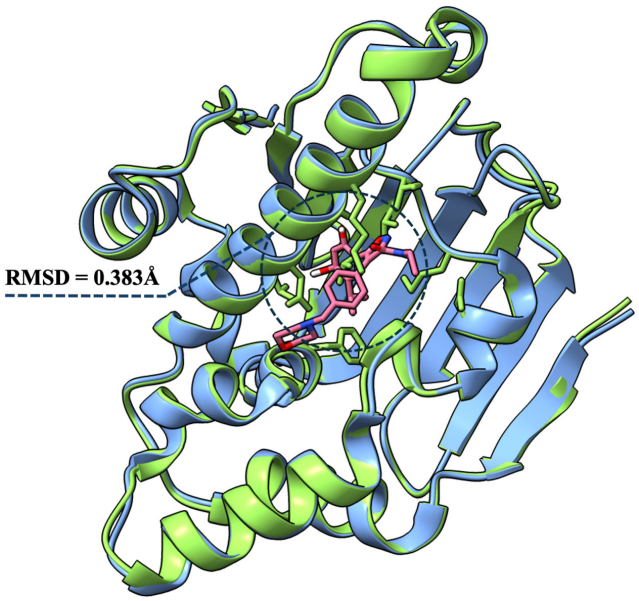

Figure 2. Solid ribbon representation of human Hsp90 (PDB ID: 6LTI) showing the alignment between the experimental (co-crystallized, green) and docked (blue) conformations of Luminespib

3.2. Prediction of small molecule binding to Hsp90

Computer-aided techniques have developed as powerful tools for predicting the macromolecular targets of bioactive small molecules [54–56]. Online prediction servers have revolutionized drug discovery by offering an efficient and rapid screening of vast chemical libraries for potential protein targets [41]. In this work, the online servers SwissTargetPredction [36], SuperPred 3.0 [37], PASS [38], and SEA [39] were utilized to conduct prediction studies for the plausibility of the identified ZINC compounds for binding to Hsp90. In this work, the potential of the identified ZINC compounds to bind Hsp90 was evaluated using online prediction servers, including SwissTargetPrediction [36], SuperPred 3.0 [37], PASS [38], and SEA [39]. *In silico* predictions consistently indicated that all selected isoxazole compounds could inhibit Hsp90 activity (Table 2). These results deliver initial understanding of the potential of these molecules as modulators of Hsp90 ATPase activity. Furthermore, considering the structural resemblance of our compounds to Luminespib, which inhibits Hsp90 by competitively occupying its ATP-binding pocket within the N-terminal domain (NTD), a similar mode of action is anticipated. Luminespib's binding to this critical site prevents ATP engagement, effectively shutting down Hsp90's ATPase activity. Consequently, this disruption leads to the destabilization and degradation of Hsp90's client proteins. By analogy, the selected molecules are predicted to possess the ability to bind within this same ATP-binding pocket, thereby disrupting Hsp90's ATPase function and its ability to stabilize oncogenic client proteins.

3.3. Evaluation of the potential for ligand inhibition via molecular docking

Molecular docking simulations were performed using the Expasy SwissDock server to examine the possible inhibitory mechanisms of chosen ZINC compounds against Hsp90. To validate our docking protocol, we performed a redocking of the co-crystallized ligand Luminespib (PDB ID: 6LTI). The resulting root-mean-square deviation (RMSD) between the docked pose and the experimental crystal structure was 0.383 Å, well below the generally accepted threshold of 2.0 Å for successful validation (Figure 2) [57]. This remarkably low RMSD value rigorously confirms the reliability and high predictive accuracy of our docking setup.

The molecular docking simulations revealed that the selected isoxazole-based compounds consistently occupy the ATP-binding pocket of Hsp90, mirroring the canonical binding mode exhibited by the co-crystallized inhibitor Luminespib (Figure 3). This conserved binding orientation underscores the ability of these compounds to establish key interactions with critical residues involved in ATP hydrolysis and chaperone activity (Table 3). The

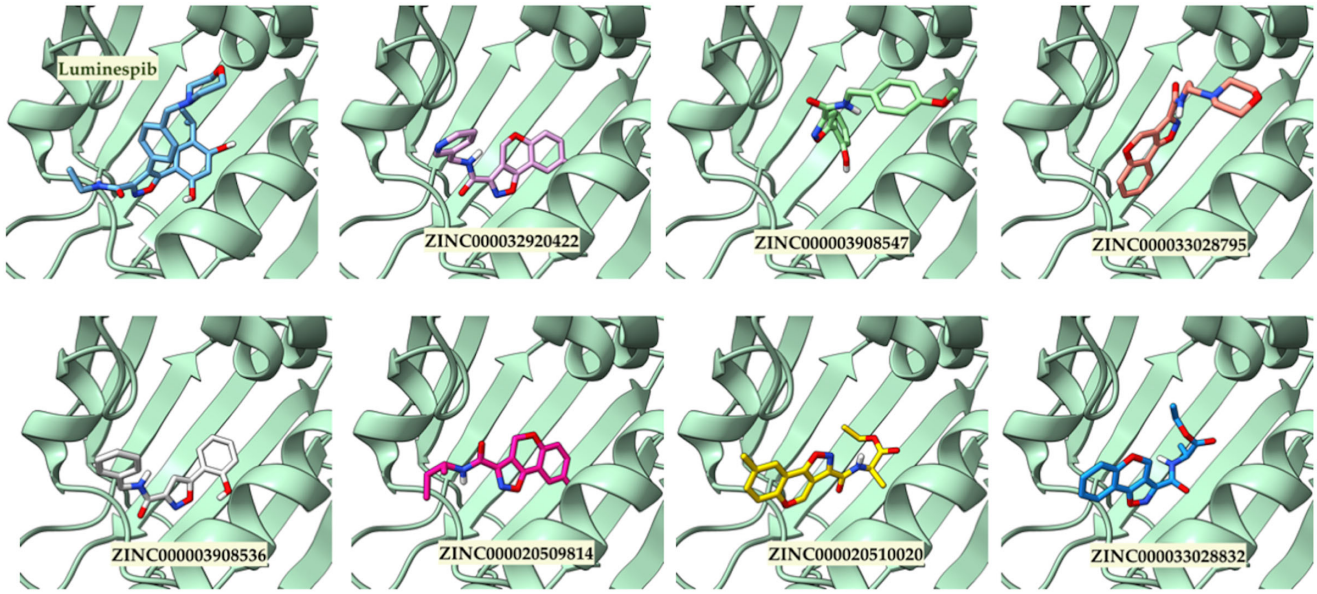

Figure 3. Ribbon representation of the Hsp90-Luminespib complex (PDB ID: 6LTI) and the predicted binding modes of top-ranked ZINC compounds within the Hsp90 ATP-binding pocket

Table 3. Lowest binding energies and interacting residues of top-ranked ZINC compounds

		Interacting Residues		
ZINC code	LBE (Kcal/mol)	Hydrogen Bond	Hydrophobic	Ionic
ZINC000032920422	−8.51	Gly97	Asn51, Lys58, Met98, Gly97, Asp93	–
ZINC000003908547	−8.42	Asp93, Gly97, Lys58	Asp93, Asn51, Asp54	–
ZINC000033028795	−8.40	Asn51, Lys58, Thr109, Phe138	Asn51, Leu107, Phe138	Asp54
ZINC000003908536	−8.37	Asp93, Gly97	Asn51, Asp93, Lys58	–
ZINC000020509814	−8.33	Gly97, Thr152, Thr184	Ala55, Thr184, Gly97, Asp93, Asn51	–
ZINC000020510020	−8.31	Gly97, Thr99, Thr109, Thr184, Thr152	Asn51, Lys58, Gly97, Gly108, Thr184	–
ZINC000033028832	−8.31	Glu47, Asn51, Lys58, Gly97, Phe138	Glu47, Phe138, Asn51	–
ZINC000020509776	−8.28	Gly97	Asn51, Lys58, Asp93, Gly97	–
ZINC000013119868	−8.27	Asn51, Thr152, Gly137	Asn51, Ala55, Gly97, Gly108, Thr109	
ZINC000033028831	−8.26	Gly97, Thr99, Met98	Asn51, Gly97, Met98	–
ZINC000020509949	−8.24	Thr184, Gly97	Met98, Lys58, Asn51,Thr184	–
ZINC000020484748	−8.23	Ser52, Gly97, Thr109, Thr152, Thr184	Asp93, Thr184, Gly97	Glu47
Luminespib	−8.20	Asn51, Asp93, Gly97, Thr152	Asn51, Phe138, Asp93	–

Table 4. Lowest binding energies of selected ZINC compounds

ZINC Compound	LBE (Kcal/mol)	ZINC Compound	LBE (Kcal/mol)
ZINC000020510095	−7.95	ZINC000020510023	−6.06
ZINC000035477380	−7.56	ZINC000003908532	−7.36
ZINC000020509814	−8.33	ZINC000003908564	−6.57
ZINC000020509816	−7.39	ZINC000003908535	−7.18
ZINC000032920495	−7.09	ZINC000033028831	−8.26
ZINC000020509949	−8.24	ZINC000033028832	−8.31
ZINC000035477309	−8.00	ZINC000033028795	−8.40
ZINC000035477310	−6.97	ZINC000003908558	−7.85
ZINC000015673863	−7.57	ZINC000013119868	−8.27
ZINC000035537827	−7.03	ZINC000013119870	−6.73
ZINC000020484607	−7.09	ZINC000032920422	−8.51
ZINC000020484604	−7.02	ZINC000003908529	−7.49
ZINC000020484847	−7.70	ZINC000003908536	−8.37
ZINC000020509776	−8.28	ZINC000003908554	−6.30
ZINC000003908545	−7.07	ZINC000003908038	−6.88
ZINC000003908546	−7.68	ZINC000047528273	−7.85
ZINC000020901917	−7.08	ZINC000003908547	−8.42
ZINC000020484748	−8.23	ZINC000020510020	−8.31
Luminespib (reference)		−8.20	

alignment of the docked isoxazole compounds with Luminespib suggests that they are capable of mimicking the pharmacophoric features necessary for effective inhibition of Hsp90's function (Figure 2) [57]. Moreover, the formation of hydrogen bonds and hydrophobic contacts with residues lining the ATP-binding cleft reinforces their potential to act as ATP-competitive inhibitors (Figures 4 and 5) [10, 58]. These findings highlight the structural compatibility of the isoxazole scaffold with the Hsp90 binding site and position these compounds as promising lead candidates for further optimization and development into potent and selective Hsp90 inhibitors. Their ability to engage the same binding site as a clinically studied inhibitor lends credence to their prospective biological relevance and therapeutic utility.

The binding energies of the selected ZINC compounds, as illustrated in Table 4, ranged from −6.30 to −8.51 kcal/mol. Of particular note, twelve compounds displayed binding energies between −8.23 and −8.51 kcal/mol, superior to that of the reference compound, Luminespib (−8.20 kcal/mol). These results imply that the selected ZINC compounds possess enhanced binding affinities for Hsp90 relative to the reference molecule, strengthening their potential as potent Hsp90 inhibitors.

An in-depth examination of the docking products showed diverse interaction styles between the top-ranked ZINC compounds and Hsp90 (Table 3, Figures 4, 5, and 6). Many of these compounds formed hydrogen bonds with Gly97, highlighting the residue's critical role in ligand recognition (Figures 4 and 5). Hydrophobic interactions with Asn51, Lys58, Asp93, and Gly97 were frequently observed, suggesting their role in stabilizing the ligand-Hsp90 complex (Figures 4 and 5).

Unique electrostatic interactions, specifically salt bridges, were observed between the Hsp90 residues Asp54, Glu47, and Asp93 (NTD) and the ZINC compounds ZINC000033028795, ZINC000020484748, and ZINC000014974852 (respectively; Table 3, Figure 6). These salt bridges are likely key determinants of ligand-protein complex specificity, stability, and affinity. At the atomic level: (i) Asp93 interacts with the hydroxyl oxygen of a phenol substituent in ZINC000014974852; (ii) Glu47 interacts with a chloride ion near a phenol substituent in ZINC000020484748;

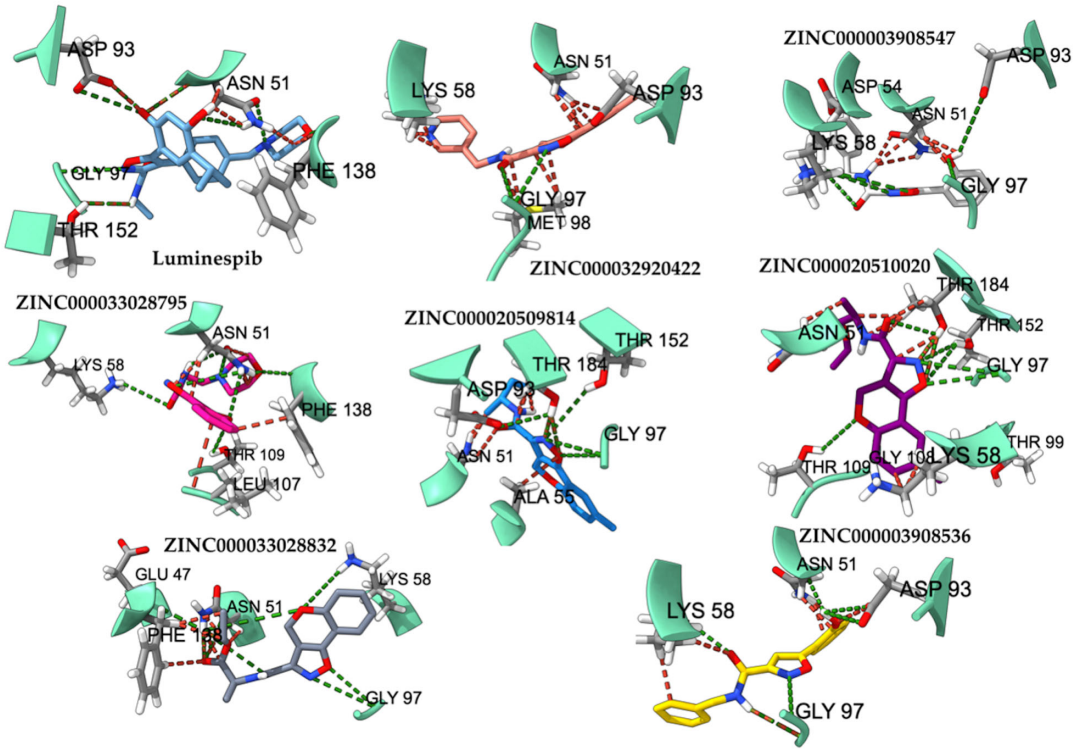

Figure 4. Ribbon representation of the Hsp90-Luminespib complex (PDB ID: 6LTI) and the predicted binding modes of the top-ranked ZINC compounds within the Hsp90 ATP-binding pocket obtained by SwissDock software, showing Hsp90 residues involved in H-bond (green line) and hydrophobic (red lines) interactions with these molecules

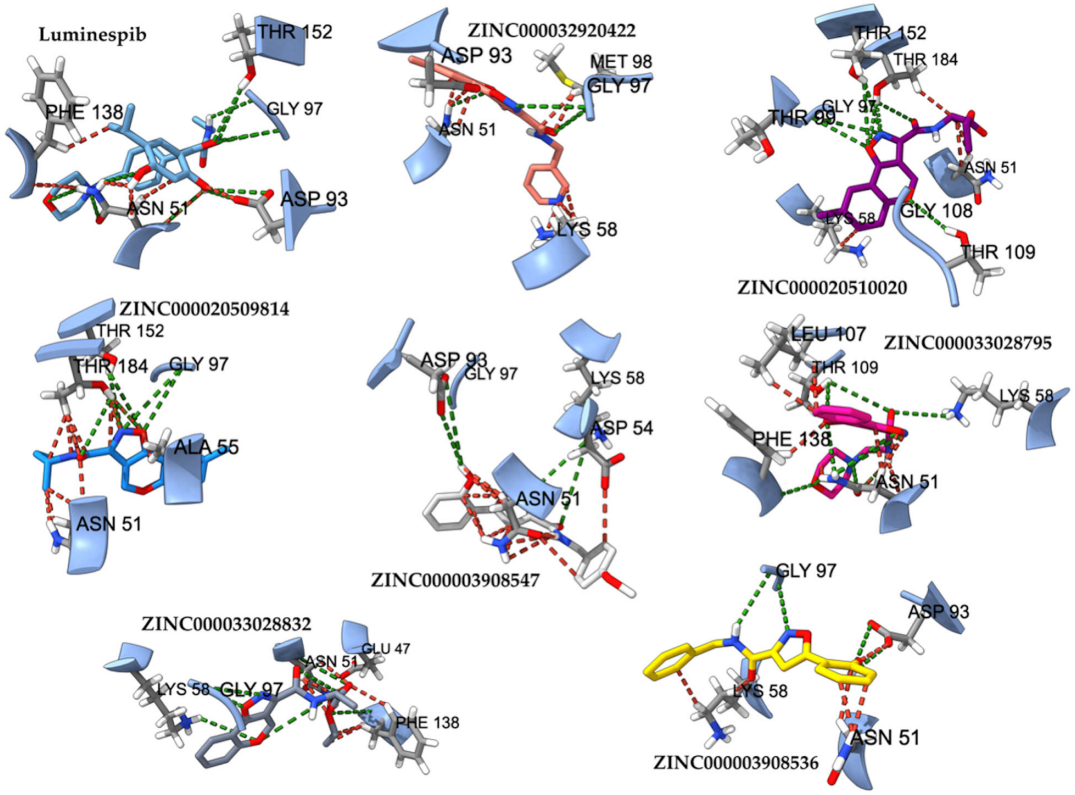

Figure 5. Stick representation of the Hsp90-Luminespib complex (PDB ID: 6LTI) and the predicted binding modes of the top-ranked ZINC compounds within the Hsp90 ATP-binding pocket obtained by AutoDock Vina 1.2.0, showing Hsp90 residues involved in H-bond (green line) and hydrophobic (red lines) interactions with these molecules

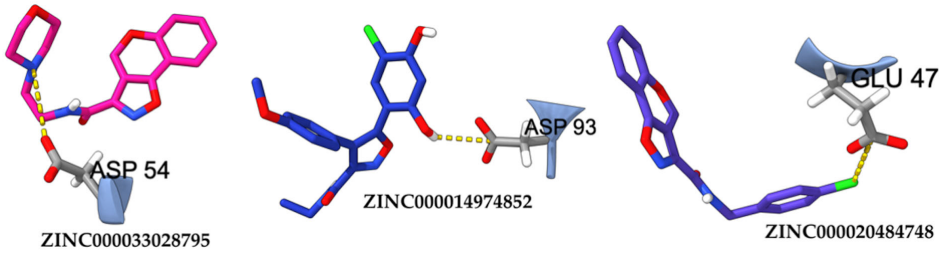

Figure 6. Electrostatic interactions between Hsp90 and ligand

and (iii) Asp54 interacts with the nitrogen atom of the morpholine moiety in ZINC000033028795. The formation of these salt bridges underscores a strategic structural complementarity between the ligands and the charged microenvironment of the Hsp90 ATP-binding site. These findings strongly suggest that incorporating polar and ionizable functional groups in ligand design can significantly enhance binding affinity, offering valuable insights to guide structure-based optimization of Hsp90 inhibitors [23].

3.4. Binding interaction pattern analysis

Luminespib exhibited diverse interactions with Hsp90, including hydrogen bonding and hydrophobic contacts involving key residues (Gly97, Asp93, Asn51, Thr152, Phe138). Similarly, top-ranked ZINC compounds, such as ZINC000032920422 and ZINC00003908547, displayed favorable binding interactions with Hsp90, characterized by hydrogen bonding and hydrophobic contacts with residues including Gly97, Asp93, Asn51, Lys58, and Met98. Notably, Asp93 and Gly97 emerged as critical for interaction with both Luminespib and these ZINC compounds, highlighting their potential as targets for future optimization. To further understand the interaction landscape of the top-ranked ZINC compounds compared to Luminespib, we performed a residue-level comparative analysis using a heatmap and a radar chart (Table 3, Figure 7). The heatmap illustrates the presence or absence of specific amino acid residues involved in binding interactions for each compound. Several residues, including Gly97, Asn51, and Asp93, were highly conserved across most compounds, suggesting their crucial role in stabilizing ligand binding within the Hsp90 pocket. Other residues, such as Thr184, Phe138, and Thr152, appeared more selectively, indicating potential for ligand-specific interactions influencing binding affinity and specificity. The radar chart provided a visual comparison of interaction profiles between Luminespib and selected high-affinity ZINC compounds, highlighting both shared interaction motifs (particularly Gly97 and Asn51) and distinct binding patterns unique to specific ZINC hits, such as additional contacts with Thr109 and Glu47. These observations are valuable for rationalizing differential binding energies and guiding future structure-based optimization efforts. Together, these visualizations emphasize the importance of conserved residues in ligand recognition and offer insight into structural features that differentiate lead-like behavior among the screened compounds.

4. Potential Biological Activities

To identify the potential biological activities of the selected ZINC compounds. A comprehensive literature and database search was conducted to investigate whether any of the 36 identified compounds have previously been tested for Hsp90-related activity. Our findings indicate that none of these compounds have been experimentally evaluated or reported as Hsp90 inhibitors to date. However, we found that 16 of the compounds were tested for other biological activities unrelated to Hsp90, and none demonstrated significant activity in those assays, suggesting that their pharmacological profiles remain largely unexplored, which reflects the potential novelty of the identified scaffolds in the context of Hsp90 inhibition and highlight the importance of future experimental validation to confirm the predicted binding affinities and mechanisms of action. To further support our findings and assess the therapeutic relevance of these compounds, we performed *in silico* cytotoxicity prediction using the CLC-Pred 2.0 platform [45]. This tool predicts cytotoxic potential in non-transformed and cancer cell lines based on structural similarities to compounds with known cytotoxic profiles. CLC-Pred 2.0 employs QSAR models trained on large

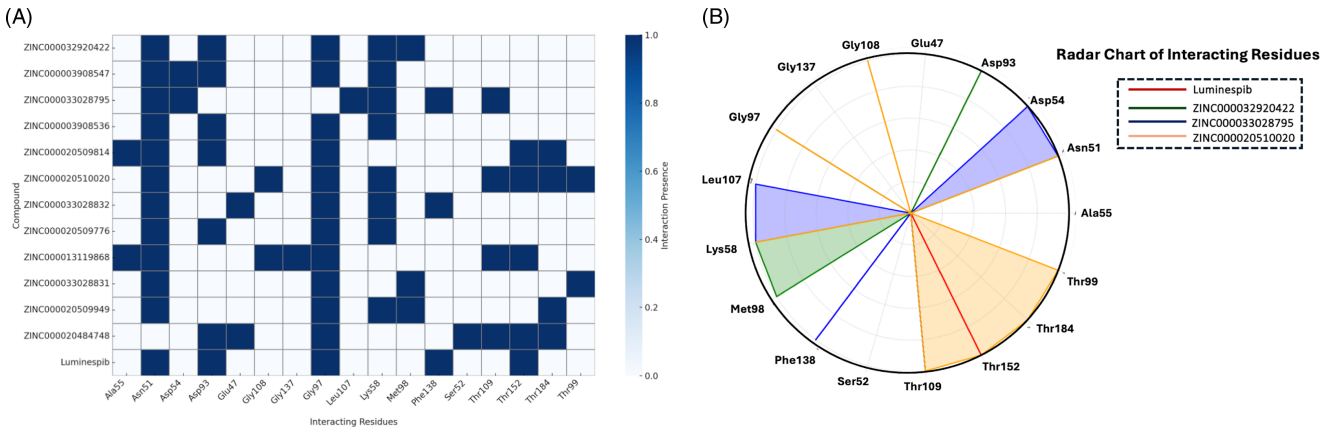

Figure 7. (A) Heatmap of residue interactions across the top-ranked ZINC compounds and Luminespib, and (B) radar chart of the interacting residues for Luminespib and the top-ranked ZINC compounds

Table 5. CLC-Pred cytotoxicity predictions for isoxazole and Luminespib

Compound	Pa*	Pi**	Cell-line	Cell-line name	Tissue/organ
ZINC000032920422	**0.556**	0.027	NCI-H838	Non-small cell lung cancer 3 stage	Lung
ZINC000003908547	**0.569**	0.005	A2780	Ovarian carcinoma	Ovarium
	0.537	0.004	HuP-T3	Pancreatic adenocarcinoma	Pancreas
ZINC000033028795	**0.574**	0.024	NCI-H838	Non-small cell lung cancer 3 stage	Lung
ZINC000003908536	**0.688**	0.004	A2780	Ovarian carcinoma	Ovarium
	0.631	0.003	HuP-T3	Pancreatic adenocarcinoma	Pancreas
ZINC000020509814	**0.553**	0.028	NCI-H838	Non-small cell lung cancer 3 stage	Lung
ZINC000020510020	**0.533**	0.034	NCI-H838	Non-small cell lung cancer 3 stage	Lung
ZINC000033028832	**0.536**	0.033	NCI-H838	Non-small cell lung cancer 3 stage	Lung
ZINC000020509776	**0.555**	0.027	NCI-H838	Non-small cell lung cancer 3 stage	Lung
ZINC000013119868	**0.585**	0.003	HuP-T3	Pancreatic adenocarcinoma	Pancreas
ZINC000033028831	**0.536**	0.033	NCI-H838	Non-small cell lung cancer 3 stage	Lung
Luminespib	**0.645**	0.014	NCI-H838	Non-small cell lung cancer 3 stage	Lung
	0.580	0.006	SK-MEL-1	Metastatic melanoma	Skin
	0.558	0.014	NCI-H460	Non-small cell lung carcinoma	Lung
	0.516	0.032	DMS-114	Lung carcinoma	Lung

Note: * Pa: Probability of Activity.
** Pi: Probability of Inactivity.

datasets of experimentally validated cytotoxicity data. The SMILES representations of our top-ranked compounds were used as input to predict their cytotoxic effects, providing a cost- and time-effective preliminary evaluation of anticancer potential and safety prior to experimental validation.

The *in silico* cytotoxicity predictions suggest that several ZINC compounds exhibit promising activity against a variety of tumor cell lines, in some cases surpassing the predicted activity of Luminespib in specific contexts (Table 5). According to CLC-Pred 2.0, Luminespib shows moderate to good, predicted cytotoxicity across several cancer cell lines, with Probability of Activity (Pa) values ranging from 0.516 to 0.645. Notably, Luminespib is predicted to be active against the NCI-H838 non-small cell lung cancer cell line (Pa = 0.645, Pi = 0.014), SK-MEL-1 metastatic melanoma (Pa = 0.580, Pi = 0.006), NCI-H460 non-small cell lung carcinoma (Pa = 0.558, Pi = 0.014), and DMS-114 lung carcinoma (Pa = 0.516, Pi = 0.032). The ZINC compounds demonstrate a range of predicted cytotoxic activities, with some compounds exceeding Luminespib's highest Pa values in certain cell lines. For example, ZINC00003908536 exhibits a Pa of 0.688 against the A2780 ovarian carcinoma cell line – higher than Luminespib's peak prediction. Additionally, several other ZINC compounds display Pa values between 0.55 and 0.60, suggesting comparable or superior predicted activity to Luminespib in select cell lines. Interestingly, both Luminespib and several ZINC compounds are predicted to be active against lung cancer cell lines, aligning with Luminespib's known anticancer activity in lung cancer. However, some ZINC compounds exhibit higher predicted activity in other tumor models, such as A2780 (ovarian carcinoma) and HuP-T3 (pancreatic adenocarcinoma), where Luminespib's activity was not reported in the dataset. This may indicate differential selectivity across tumor types. Importantly, the low Probability of Inactivity (Pi) values observed for both Luminespib and the ZINC compounds further support their potential efficacy. While these computational predictions provide encouraging preliminary evidence for anticancer activity, experimental validation is essential to confirm their mechanisms of action and evaluate their viability as therapeutic candidates.

5. Conclusion and Future Direction

Breakthroughs in deep learning technologies have established *in silico* approaches as versatile and reliable tools in all stages of drug discovery, from small molecule screening to examining potential biological activities [15, 30, 31]. Computer-aided techniques were employed in this study to identify isoxazole-based molecules as potential inhibitors of Hsp90 oncogenic activity, guided by the structure of the third-generation Hsp90 inhibitor, Luminespib. Of the 400 top-ranked ZINC compounds, 36 were selected for further investigation via target prediction online servers and molecular docking simulation. The shortlisted molecules demonstrated potential for Hsp90 inhibition. Furthermore, twelve of these compounds exhibited superior binding affinities for Hsp90 compared to the control compound, Luminespib. Molecular docking simulations revealed that a combination of hydrogen bonds and hydrophobic interactions with Hsp90 critical residues such as Asp93, Gly97, Asn51, and Lys58 drives the potential activity of these ZINC compounds. Further investigation of the role of these residues in modulating Hsp90 activity and optimizing these compounds' structural and pharmacokinetic properties could lead to novel, effective anticancer agents targeting this chaperone machinery. Finally, to comprehensively validate their potential in halting cancer cell proliferation, conducting thorough investigations using cell-based and *in vivo* models and optimizing dosing regimens is imperative.

Acknowledgement

The author acknowledges that an earlier version of this manuscript was published as a preprint at Research Square (DOI: 10.21203/rs.3.rs-4542530/v1) on 9 June, 2024. The preprint has not been peer reviewed. This published article incorporates revisions made during the peer review process for *Medinformatics*.

Conflicts of Interest

The author declares that he has no conflicts of interest to this work.

Data Availability Statement

Data sharing is not applicable to this article as no new data were created or analyzed in this study.

Author Contribution Statement

Adam A. Aboalroub: Conceptualization, Methodology, Software, Validation, Formal analysis, Investigation, Data curation, Writing – original draft, Writing – review & editing, Visualization, Supervision, Project administration.

References

[1] Brown, J. S., Amend, S. R., Austin, R. H., Gatenby, R. A., Hammarlund, E. U., & Pienta, K. J. (2023). Updating the definition of cancer. *Molecular Cancer Research*, *21*(11), 1142–1147. https://doi.org/10.1158/1541-7786.MCR-23-0411

[2] Che, J., Song, R., Chen, B., & Dong, X. (2020). Targeting CXCR1/2: The medicinal potential as cancer immunotherapy agents, antagonists research highlights and challenges ahead. *European Journal of Medicinal Chemistry*, *185*, 111853. https://doi.org/10.1016/j.ejmech.2019.111853

[3] de Visser, K. E., & Joyce, J. A. (2023). The evolving tumor microenvironment: From cancer initiation to metastatic outgrowth. *Cancer Cell*, *41*(3), 374–403. https://doi.org/10.1016/j.ccell.2023.02.016

[4] Hoter, A., El-Sabban, M. E., & Naim, H. Y. (2018). The HSP90 family: Structure, regulation, function, and implications in health and disease. *International Journal of Molecular Sciences*, *19*(9), 2560. https://doi.org/10.3390/ijms19092560

[5] Wei, H., Zhang, Y., Jia, Y., Chen, X., Niu, T., Chatterjee, A., . . . , & Hou, G. (2024). Heat shock protein 90: Biological functions, diseases, and therapeutic targets. *MedComm*, *5*(2), e470. https://doi.org/10.1002/mco2.470

[6] Jafari, A., Rezaei-Tavirani, M., Farhadihosseinabadi, B., Taranejoo, S., & Zali, H. (2020). HSP90 and co-chaperones: Impact on tumor progression and prospects for molecular-targeted cancer therapy. *Cancer Investigation*, *38*(5), 310–328. https://doi.org/10.1080/07357907.2020.1752227

[7] Woodford, M. R., Backe, S. J., Sager, R. A., Bourboulia, D., Bratslavsky, G., & Mollapour, M. (2021). The role of heat shock protein-90 in the pathogenesis of Birt-Hogg-Dubé and tuberous sclerosis complex syndromes. *Urologic Oncology: Seminars and Original Investigations*, *39*(6), 322–326. https://doi.org/10.1016/j.urolonc.2020.03.016

[8] Keshavarzipour, F., Abbasi, M., Khorsandi, Z., Ardestani, M., & Sadeghi-Aliabadi, H. (2024). Design, synthesis and biological studies of new isoxazole compounds as potent Hsp90 inhibitors. *Scientific Reports*, *14*(1), 28017. https://doi.org/10.1038/s41598-024-79051-5

[9] Ren, X., Li, T., Zhang, W., & Yang, X. (2022). Targeting heat-shock protein 90 in cancer: An update on combination therapy. *Cells*, *11*(16), 2556. https://doi.org/10.3390/cells11162556

[10] Poyya, J., & Joshi, C. G. (2024). *Inhibition of the HSP90 homodimerization and HSP90-HIF1α interactions by employing small molecules at C-terminal ATP binding site of HSP90*. bioRxiv. https://doi.org/10.1101/2024.06.02.595921

[11] Li, Z. N., & Luo, Y. (2023). HSP90 inhibitors and cancer: Prospects for use in targeted therapies. *Oncology Reports*, *49*(1), 6. https://doi.org/10.3892/or.2022.8443

[12] Kaplan, Ö., & Gökşen Tosun, N. (2024). Molecular pathway of anticancer effect of next-generation HSP90 inhibitors XL-888 and Debio0932 in neuroblastoma cell line. *Medical Oncology*, *41*(8), 194. https://doi.org/10.1007/s12032-024-02428-z

[13] Rehman, M. U., He, F., Shu, X., Guo, J., Liu, Z., Cao, S., & Long, S. (2024). Antibacterial and antifungal pyrazoles based on different construction strategies. *European Journal of Medicinal Chemistry*, *282*, 117081. https://doi.org/10.1016/j.ejmech.2024.117081

[14] Kabir, E., & Uzzaman, M. (2022). A review on biological and medicinal impact of heterocyclic compounds. *Results in Chemistry*, *4*, 100606. https://doi.org/10.1016/j.rechem.2022.100606

[15] Aboalroub, A. A., & Al-Najjar, B. O. (2024). In-silico identification of 3, 4-Diarylpyrazoles-based small molecules as potential Hsp90 inhibitors. *Results in Chemistry*, *11*, 101757. https://doi.org/10.1016/j.rechem.2024.101757

[16] Kumar, M. V. V., Noor, R. E., Davis, R. E., Zhang, Z., Sipavicius, E., Keramisanou, D., . . . , & Gelis, I. (2018) Molecular insights into the interaction of Hsp90 with allosteric inhibitors targeting the C-terminal domain. *MedChemComm*, *9*(8), 1323–1331. https://doi.org/10.1039/C8MD00151K

[17] Aboalroub, A. A., Zhang, Z., Keramisanou, D., & Gelis, I. (2017). Backbone resonance assignment of an insect arylalkylamine *N*-acetyltransferase from *Bombyx mori* reveals conformational heterogeneity. *Biomolecular NMR Assignments, 11*(1), 105–109. https://doi.org/10.1007/s12104-017-9729-8

[18] Li, J., & Zhang, J. (2022). The antibacterial activity of 1, 2, 3-triazole- and 1, 2, 4-triazole-containing hybrids against *Staphylococcus aureus*: An updated review (2020-present). *Current Topics in Medicinal Chemistry, 22*(1), 41–63. https://doi.org/10.2174/1568026621666211111160332

[19] Tian, G., Song, Q., Liu, Z., Guo, J., Cao, S., & Long, S. (2023). Recent advances in 1, 2, 3- and 1, 2, 4-triazole hybrids as antimicrobials and their SAR: A critical review. *European Journal of Medicinal Chemistry*, *259*, 115603. https://doi.org/10.1016/j.ejmech.2023.115603

[20] McDonald, E., Jones, K., Brough, P. A., Drysdale, M. J., & Workman, P. (2006). Discovery and development of pyrazole-scaffold Hsp90 inhibitors. *Current Topics in Medicinal Chemistry*, *6*(11), 1193–1203. https://doi.org/10.2174/156802606777812086

[21] Sharp, S. Y., Prodromou, C., Boxall, K., Powers, M. V., Holmes, J. L., Box, G., . . . , & Workman, P. (2007). Inhibition of the heat shock protein 90 molecular chaperone *in vitro* and *in vivo* by novel, synthetic, potent resorcinylic pyrazole/isoxazole amide analogues. *Molecular Cancer Therapeutics*, *6*(4), 1198–1211. https://doi.org/10.1158/1535-7163.MCT-07-0149

[22] Wang, X., Hu, Q., Tang, H., & Pan, X. (2023). Isoxazole/isoxazoline skeleton in the structural modification of natural products: A review. *Pharmaceuticals*, *16*(2), 228. https://doi.org/10.3390/ph16020228

[23] Magwenyane, A. M., Lawal, M. M., Amoako, D. G., Somboro, A. M., Agoni, C., Khan, R. B., . . . , & Kumalo, H. M. (2022).

Exploring the inhibitory mechanism of resorcinylic isoxazole amine NVP-AUY922 towards the discovery of potential heat shock protein 90 (Hsp90) inhibitors. *Scientific African*, *15*, e01107. https://doi.org/10.1016/j.sciaf.2022.e01107

[24] Li, Z. N., & Luo, Y. (2023). HSP90 inhibitors and cancer: Prospects for use in targeted therapies. *Oncology Reports*, *49*(1), 6. https://doi.org/10.3892/or.2022.8443

[25] Ardestani, M., Khorsandi, Z., Keshavarzipour, F., Iravani, S., Sadeghi-Aliabadi, H., & Varma, R. S. (2022). Heterocyclic compounds as Hsp90 inhibitors: A perspective on anticancer applications. *Pharmaceutics*, *14*(10), 2220. https://doi.org/10.3390/pharmaceutics14102220

[26] Fang, X., Feng, J., Wang, K., & Luan, Y. (2023). Development of VER-50589 analogs as novel Hsp90 inhibitors. *Bioorganic & Medicinal Chemistry Letters*, *91*, 129375. https://doi.org/10.1016/j.bmcl.2023.129375

[27] Epp-Ducharme, B., Dunne, M., Fan, L., Evans, J. C., Ahmed, L., Bannigan, P., & Allen, C. (2021). Heat-activated nanomedicine formulation improves the anticancer potential of the HSP90 inhibitor luminespib in vitro. *Scientific Reports*, *11*(1), 11103. https://doi.org/10.1038/s41598-021-90585-w

[28] Jung, J., Kwon, J., Hong, S., Moon, A. N., Jeong, J., Kwon, S., . . . , & Lee, J. (2020). Discovery of novel heat shock protein (Hsp90) inhibitors based on luminespib with potent antitumor activity. *Bioorganic & Medicinal Chemistry Letters*, *30*(12), 127165. https://doi.org/10.1016/j.bmcl.2020.127165

[29] Aboalroub, A. (2025). In silico *identification of spirodioxynaphthalenes as promising Hsp90 inhibitors*. Research Square. https://doi.org/10.21203/rs.3.rs-6199117/v1

[30] Brogi, S., Ramalho, T. C., Kuca, K., Medina-Franco, J. L., & Valko, M. (2020). Editorial: *In silico* methods for drug design and discovery. *Frontiers in Chemistry*, *8*, 612. https://doi.org/10.3389/fchem.2020.00612

[31] Gürdere, M. B., Budak, Y., Kocyigit, U. M., Taslimi, P., Tüzün, B., & Ceylan, M. (2021). ADME properties, bioactivity and molecular docking studies of 4-amino-chalcone derivatives: New analogues for the treatment of Alzheimer, glaucoma and epileptic diseases. *In Silico Pharmacology*, *9*(1), 34. https://doi.org/10.1007/s40203-021-00094-x

[32] Zoete, V., Daina, A., Bovigny, C., & Michielin, O. (2016). SwissSimilarity: A web tool for low to ultra high throughput ligand-based virtual screening. *Journal of Chemical Information and Modeling, 56*(8), 1399–1404. https://doi.org/10.1021/acs.jcim.6b00174

[33] Bragina, M. E., Daina, A., Perez, M. A. S., Michielin, O., & Zoete, V. (2022). The SwissSimilarity 2021 web tool: Novel chemical libraries and additional methods for an enhanced ligand-based virtual screening experience. *International Journal of Molecular Sciences*, *23*(2), 811. https://doi.org/10.3390/ijms23020811

[34] Lipinski, C. A. (2004). Lead- and drug-like compounds: The rule-of-five revolution. *Drug Discovery Today: Technologies*, *1*(4), 337–341. https://doi.org/10.1016/j.ddtec.2004.11.007

[35] Daina, A., Michielin, O., & Zoete, V. (2017). SwissADME: A free web tool to evaluate pharmacokinetics, drug-likeness and medicinal chemistry friendliness of small molecules. *Scientific Reports*, *7*(1), 42717. https://doi.org/10.1038/srep42717

[36] Gfeller, D., Grosdidier, A., Wirth, M., Daina, A., Michielin, O., & Zoete, V. (2014). SwissTargetPrediction: A web server for target prediction of bioactive small molecules. *Nucleic Acids Research*, *42*(W1), W32–W38. https://doi.org/10.1093/nar/gku293

[37] Gallo, K., Goede, A., Preissner, R., & Gohlke, B. O. (2022). SuperPred 3.0: Drug classification and target prediction–A machine learning approach. *Nucleic Acids Research*, *50*(W1), W726–W731. https://doi.org/10.1093/nar/gkac297

[38] Lagunin, A., Stepanchikova, A., Filimonov, D., & Poroikov, V. (2000). PASS: Prediction of activity spectra for biologically active substances. *Bioinformatics*, *16*(8), 747–748. https://doi.org/10.1093/bioinformatics/16.8.747

[39] Wang, Z., Liang, L., Yin, Z., & Lin, J. (2016). Improving chemical similarity ensemble approach in target prediction. *Journal of Cheminformatics, 8*(1), 20. https://doi.org/10.1186/s13321-016-0130-x

[40] Morris, G. M., Goodsell, D. S., Halliday, R. S., Huey, R., Hart, W. E., Belew, R. K., & Olson, A. J. (1998). Automated docking using a Lamarckian genetic algorithm and an empirical binding free energy function. *Journal of Computational Chemistry*, *19*(14), 1639–1662. https://doi.org/10.1002/(SICI)1096-987X(19981115)19:14%3C1639::AID-JCC10%3E3.0.CO;2-B

[41] Morris, G. M., Huey, R., Lindstrom, W., Sanner, M. F., Belew, R. K., Goodsell, D. S., & Olson, A. J. (2009). AutoDock4 and AutoDockTools4: Automated docking with selective receptor flexibility. *Journal of Computational Chemistry*, *30*(16), 2785–2791. https://doi.org/10.1002/jcc.21256

[42] Grosdidier, A., Zoete, V., & Michielin, O. (2011). SwissDock, a protein-small molecule docking web service based on EADock DSS. *Nucleic Acids Research*, *39*(suppl_2), W270–W277. https://doi.org/10.1093/nar/gkr366

[43] Pettersen, E. F., Goddard, T. D., Huang, C. C., Couch, G. S., Greenblatt, D. M., Meng, E. C., & Ferrin, T. E. (2004). UCSF Chimera–A visualization system for exploratory research and analysis. *Journal of Computational Chemistry*, *25*(13), 1605–1612. https://doi.org/10.1002/jcc.20084

[44] Irwin, J. J., Sterling, T., Mysinger, M. M., Bolstad, E. S., & Coleman, R. G. (2012). ZINC: A free tool to discover chemistry for biology. *Journal of Chemical Information and Modeling*, *52*(7), 1757–1768. https://doi.org/10.1021/ci3001277

[45] Lagunin, A. A., Rudik, A. V., Pogodin, P. V., Savosina, P. I., Tarasova, O. A., Dmitriev, A. V., . . . , & Poroikov, V. V. (2023). CLC-Pred 2.0: A freely available web application for in silico prediction of human cell line cytotoxicity and molecular mechanisms of action for druglike compounds. *International Journal of Molecular Sciences*, *24*(2), 1689. https://doi.org/10.3390/ijms24021689

[46] Aboalroub, A. A., & Al Azzam, K. M. (2024). Protein S-Nitrosylation: A chemical modification with ubiquitous biological activities. *The Protein Journal*, *43*(4), 639–655. https://doi.org/10.1007/s10930-024-10223-y

[47] Newman, D. J., & Cragg, G. M. (2020). Natural products as sources of new drugs over the nearly four decades from 01/1981 to 09/2019. *Journal of Natural Products*, *83*(3), 770–803. https://doi.org/10.1021/acs.jnatprod.9b01285

[48] Avendaño, C., & Menéndez, J. C. (2023). Miscellaneous small- molecule and biological approaches to targeted cancer therapy. In C. Avendano & J. C. Menéndez (Eds.), *Medicinal chemistry of anticancer drugs* (3rd ed., pp. 743–822). Elsevier. https://doi.org/10.1016/B978-0-12-818549-0.00016-9

[49] Serwetnyk, M. A., & Blagg, B. S. J. (2021). The disruption of protein–protein interactions with co-chaperones and client substrates as a strategy towards Hsp90 inhibition. *Acta Pharmaceutica Sinica B*, *11*(6), 1446–1468. https://doi.org/10.1016/j.apsb.2020.11.015

[50] Duran-Frigola, M., Pauls, E., Guitart-Pla, O., Bertoni, M., Alcalde, V., Amat, D., . . . , & Aloy, P. (2020). Extending the small-molecule similarity principle to all levels of biology with the Chemical Checker. *Nature Biotechnology*, *38*(9), 1098. https://doi.org/10.1038/s41587-020-0564-6

[51] Shen, J., Cheng, F., Xu, Y., Li, W., & Tang, Y. (2010). Estimation of ADME properties with substructure pattern recognition. *Journal of Chemical Information and Modeling*, *50*(6), 1034–1041. https://doi.org/10.1021/ci100104j

[52] Keiser, M. J., Roth, B. L., Armbruster, B. N., Ernsberger, P., Irwin, J. J., & Shoichet, B. K. (2007). Relating protein pharmacology by ligand chemistry. *Nature Biotechnology*, *25*(2), 197–206. https://doi.org/10.1038/nbt1284

[53] Shin, H. K., Kang, Y.-M., & No, K. T. (2017). Predicting ADME properties of chemicals. In J. Leszczynski (Ed.), *Handbook of computational chemistry* (pp. 1–37). Springer. https://doi.org/10.1007/978-3-319-27282-5_59

[54] Zhao, Q., Ma, J., Xie, F., Wang, Y., Zhang, Y., Li, H., . . . , & Han, K. (2021). Recent advances in predicting protein S-nitrosylation sites. *BioMed Research International*, *2021*(1), 5542224. https://doi.org/10.1155/2021/5542224

[55] Li, H., Sun, X., Cui, W., Xu, M., Dong, J., Ekundayo, B. E., . . . , & Vogel, H. (2024). Computational drug development for membrane protein targets. *Nature Biotechnology*, *42*(2), 229–242. https://doi.org/10.1038/s41587-023-01987-2

[56] Vemula, D., Jayasurya, P., Sushmitha, V., Kumar, Y. N., & Bhandari, V. (2023). CADD, AI and ML in drug discovery: A comprehensive review. *European Journal of Pharmaceutical Sciences*, *181*, 106324. https://doi.org/10.1016/j.ejps.2022.106324

[57] Hevener, K. E., Zhao, W., Ball, D. M., Babaoglu, K., Qi, J., White, S. W., & Lee, R. E. (2009). Validation of molecular docking programs for virtual screening against dihydropteroate synthase. *Journal of Chemical Information and Modeling*, *49*(2), 444–460. https://doi.org/10.1021/ci800293n

[58] Nobili, S., Lapucci, A., Landini, I., Coronnello, M., Roviello, G., & Mini, E. (2020). Role of ATP-binding cassette transporters in cancer initiation and progression. *Seminars in Cancer Biology, 60*, 72–95. https://doi.org/10.1016/j.semcancer.2019.08.006

How to Cite: Aboalroub, A. A. (2025). Virtual Screening and Molecular Docking Characterization of Isoxazole-Based Small Molecules as Potential Hsp90 Inhibitors: An in Silico Insight. *Medinformatics*, *2*(3), 154–166. https://doi.org/10.47852/bonviewMEDIN52025019